Diagnostic of head blight and leaf blotch diseases of wheat in Sweden using a mycobiome isolation approach

2024_02_25

Harleen Kaur [1,*], Elisa Vilvert [1,*], Miguel Ángel Corrales Gutiérrez [1], Jiasui Zhan [1], Dimitar Douchkov [2], Francesca Desiderio [3], Heriberto Vélëz [1,4], Salim Bourras [1].

[1] Department of Forest Mycology and Plant Pathology. Swedish University of Agricultural Sciences. Almas Allé 5, 750 07, Uppsala, Sweden.

[2] Leibniz-Institute of Plant Genetics and Crop Plant Research (IPK), 06466-Gatersleben, Germany.

[3] Council for Agricultural Research and Economics (CREA) - Research Centre for Genomics and Bioinformatics, Fiorenzuola d'Arda, Italy

[4] Current address: College of Science, Mathematics and Technology. Wenzhou-Kean University. 88 Daxue Rd, Ouhai, Wenzhou, Zhejiang Province 325060, China.

*** Correspondence:**
Dr. Heriberto Vélëz

hvelez@kean.edu

Prof. Dr. Salim Bourras

salim.bourras@slu.se

Keywords: wheat, Fusarium head blight, FHB, leaf botch, mycobiome

Abstract

Increasing the durability of crop resistance to plant pathogens has become a major concern in plant pathology. There are 32 diseases of agronomical importance in wheat, which makes disease management in this crop of worldwide importance extremely challenging. Two important groups of wheat pathogens driving the consumption of chemical fungicides in Sweden and worldwide are those causing head blight diseases and leaf blotch diseases. Swedish fields are regularly infested with head blight diseases typically driven by a complex of *Fusarium* and non-fusarium taxa including *F. graminearum*, *F. culmorum*, while leaf blotches are typically caused by *Zymoseptoria tritici*, *Pyrenophora tritici-repentis*, and *Parastagonospora nodorum*. In this work, we present a survey of the larger diversity of taxa associated with head blight and leaf blotch diseases in Sweden, with the primary aim to assess the usefulness of such an approach to develop new understanding and tools for disease diagnostics and management *sensu lato*. Here, we analyze nearly a thousand isolates collected from wheat fields across eight counties in Sweden and report the identification of pathogenic and non-pathogenic taxa as well as candidate biological control agents associated with head blight and leaf blotch diseases. We argue that such surveys represent an important tool for improving disease diagnostics, disease forecasting, and integrated management in wheat.

Introduction

Disease identification in the field can be very challenging, considering the complexity and the convergence of symptoms caused by different pathogen species. For diseases typically caused by a complex such as Fusarium Head Blight (FHB), several fungal species can be implicated. For instance, there are 17 *Fusarium* sp. and non-*Fusarium* species implicated in FHB. Of these, *F. graminearum* and *F. culmorum* are often presented as the most important drivers of the disease, with F. *graminearum* often being the most predominant species (**Karlsson et al., 2021**). The composition of the complex can significantly vary among countries depending on the varieties grown in the field, agricultural practices, or climate (**Karlsson et al., 2021**). For instance, a field monitoring study conducted by Xu et al. (2005) in four European countries (Hungary, Ireland, Italy, and the UK), it was shown that FHB was frequently associated with *F. graminearum* and *F. poae* in Italy and Hungary but not in Ireland and the UK, while *F. culmorum* was rarely detected except in Ireland (**Xu et al., 2005**). This demonstrates the importance of regularly monitoring FHB for the correct identification of the causal agents and proper assessing the efficiency of management strategies.

Other prominent examples of phenotypic complexity are leaf blotch diseases caused by *Zymoseptoria tritici*, *Pyrenophora tritici-repentis*, and *Parastagonospora nodorum*. All pathogens cause convergent disease symptoms that can be confounded with each other. Actually, the three pathogen species were historically confounded as one species, then *Z. tritici* and *P. nodorum* were referred to as the Septoria blotch complex or Septoria complex due to frequent co-occurrence of the two species and the similarity of symptoms. From a resistance breeding perspective, the distinction between those three species is crucial since it was shown that the host resistance is genetically different (i.e., requires different resistance genes, resistance mechanisms, and breeding strategies) (**Brown et al., 2015**). This further demonstrates the importance of monitoring and precise disease diagnostics as a tool for disease management. Furthermore, leaf blotch diseases in wheat are still largely controlled with fungicides, leading to the rapid development of fungicide resistance in pathogen populations across Europe (**Pereira et al., 2020; Justesen et al., 2021; Jørgensen et al., 2021, Jørgensen et al., 2022**) Thus, surveys are essential for the management of fungicide resistance and further highlight the importance of continuous isolation and characterization of pathogen populations from the field.

66 One major challenge for disease diagnosis in wheat is the recurrent emergence of hypervirulent
67 pathogen races, with one prominent example being the stem UG99 from the wheat pathogen *Puccinia*
68 *graminis* f. sp. *tritici*, that was responsible for a global pandemic of stem rust in wheat (**Singh et al.,**
69 **2011**). From a phenotypic perspective, it is impossible to distinguish the stem rust symptoms caused
70 by the UG99 race from any other race, thus highlighting the importance of molecular race
71 characterization for proper monitoring and resistance breeding (**Patpour et al., 2022**). A similar
72 challenge is imposed by *Blumeria graminis* f.sp. *triticale* (*B.g. triticale*), a new wheat pathogen that
73 emerged from the hybridization of wheat powdery mildew (*B.g. tritici*) and rye powdery mildew (*B.g.*
74 *secalis*) (**Menardo et al., 2016**). *B.g. triticale* is a new pathogen with an expanded host range that can
75 not only infect the Triticale crop but also wheat, causing symptoms that are indistinguishable from the
76 native wheat powdery mildew species *B.g. tritici* (**Menardo et al., 2016**) These examples further
77 demonstrate the importance of monitoring and the molecular identification of the causal agent as a tool
78 for the surveillance of emerging and re-emerging diseases.

79

80 The wheat mycobiome has been shown to be an important source of beneficial fungal endophytes with
81 promising biological control properties. Such antagonists often occur in the same ecological
82 niches/tissues as their 'target' pathogen species and have thus been isolated from various organs,
83 including roots, leaves, seeds, or ears (**Huang & Pang, 2017; Yue et al., 2018; Rojas et al., 2020**).
84 Considering the genetic diversity of the endophytic taxa inhabiting wheat, only a fraction of the wheat
85 mycobiome has been characterized for its biological control properties. Such work is mainly restricted
86 by the tedious initial isolation and molecular characterization of hundreds (if not thousands) of fungal
87 taxa. We, therefore, argue that surveys for diseases could be coupled with surveys for biological control
88 agents, taking advantage of the availability of host tissues where both pathogens and potential
89 antagonists can be isolated. In this study, we aimed to provide an experimental proof-of-concept for
90 the possible uses of disease sampling and monitoring campaigns for constructing a wheat mycobiome
91 library that can be used to understand and monitor wheat head blight and leaf blotch diseases in
92 Sweden. In particular, we assess if such a library can inform on shifts in pathogen populations and
93 possibly lead to the identification of potential emerging diseases and candidate biological control
94 agents.
95

Materials and methods

Sample collection and handling

A survey of wheat diseases was conducted in collaboration with the plant protection extension services of the Swedish Board of Agriculture. In 2020, spikes were collected from spring wheat varieties cultivated in Sweden and grown in a small propagation plot north of Stockholm. The plot consisted of the six Spring wheat varieties: Alderon, Dacke, Dala, Happy, Rohan, Stanley; two spring wheat genotypes used as scientific standards: Bobwhite and Fielder; and one triticale genotype. In 2021 and 2023, spike and leaf samples were collected by field pathologists from the plant protection extension services from eight counties across Sweden: Norrbotten, Uppsala, Stockholm, Södermanlands, Östergötland, Västra Götaland, Gottland, and Skåna (Figure 1 A). Samples were typically shipped within 24 hours in glycine bags and immediately processed or stored at 4°C in dry storage until further processing.

Media preparation for isolation and long-term conservation

Two different media were used for pathogen isolation, purification, and long-term storage. Potato dextrose agar (PDA) was prepared from dehydrated pre-mixed media from MP Biomedicals (USA) according to the manufacturer's instructions. Yeast malt sucrose (YMS) agar medium was prepared by mixing solve 4 g yeast extract, 4 g malt extract, and 4 g sucrose, and 16 g agar in 1000 ml milliQ water, then autoclaving for 5 min at 121°C. For mid-term storage, isolates were kept as slow-growing cultures on half-strength PDA or YMS agar in small glass vials and stored in the dark at 4°C. For long-term storage, three to four ca, 5mm mycelial plugs were cut from a growing colon, placed in a 2ml cryotube containing 30% glycerol, and stored at -80°C. For *Z. tritici*, long-term storage vials were prepared from liquid cultures as previously described by Fagundes and collaborators (**Fagundes et al., 2020**).

Isolation and purification of fungal colonies from spikes and leaves

Seeds and glumes were manually separated from full spikes and surface sterilized under a sterile hood for one minute in 1% sodium hypochlorite, followed by 30 seconds in 70% ethanol, and washed twice for 30 seconds in autoclaved Milli-Q water. Individual seeds were placed in Petri plates containing fungal culture media amended with 50 µg/ml of Kanamycin. For leaf segments a square of ca 5mm width was dissected around blotch symptoms typically consisting of necrotic spot often surrounded by

126 a chlorotic ring. Segments were surface sterilized under a sterile hood for 30 seconds in sodium
127 hypochlorite, followed by 30 seconds in 70% ethanol, and washed twice for 30 seconds in autoclaved
128 Milli-Q water. Three samples from the same leaf were placed in Petri plates containing fungal culture
129 media amended with 50 µg/ml of Kanamycin. Alternatively, samples were also simply washed in Milli-
130 Q water and further processed into plating. All plates were incubated at 20°C until colonies were visible
131 (usually around 5 to 7 days). Individual colonies were picked and transferred to new plates and
132 incubated at 20°C. The process was repeated until a single pure colony was obtained. For the specific
133 case of *Z. tritici*, leaf segments harboring pycnidia were incubated at 18°C in a humid chamber
134 consisting of a Petri dish supplemented with a sterile absorbent paper disk soaked with sterile water.
135 Plates were inspected every day under a binocular to search for bursting pycnidia where mucilage had
136 been ejected. In such a case, the pycnidium was carefully fetched using a sterile needle under a
137 binocular placed inside a sterile hood and transferred into a Petri dish with YMS agar, supplemented
138 with 50 µg/ml of Kanamycin.

139

140 **DNA extraction and genotyping by fragment sequencing**

141 A modified cetyltrimethylammonium bromide (CTAB) based DNA extraction method was used to
142 extract DNA of fungal isolates. Briefly, mycelium plugs were used to inoculate a liquid medium
143 containing malt extracts and vitamins (MEV). Cultures were incubated with ca. 150rpm shaking in the
144 dark at 25°C for two weeks. Then, mycelium was harvested, homogenized with a CTAB buffer (3%
145 CTAB; 150 mM TRIS-HCl; 2.6 M NaCl; 20 mM EDTA), and incubated at 65°C for 30 min inside a
146 water bath. The samples were centrifuged at 10’000 g for 10 min and the supernatant was transferred
147 to a new tube supplemented with an equal volume of chloroform. After a second centrifugation at
148 10’000 g for 10 min, the supernatant was transferred to a new tube, an equal amount of isopropanol
149 was added, and the mix was incubated at -20°C for a few minutes. A final centrifugation at 10’000 g
150 for 10 min resulted in the deposition of a DNA pellet, which was washed using 70% ethanol and
151 resuspended in TE buffer. In addition, another DNA extraction method was used to extract the DNA
152 of the fungal isolates. First, mycelium plugs from the isolates were cultured in falcon tubes containing
153 10 ml of YMS liquid medium and incubated for 7-15 days at 150 rpm and 25 °C in dark. Then, the
154 mycelium was harvested, freeze-dried, and subjected to genomic DNA extraction using the Nucleo
155 Mag Plant kit (Macherey-Nagel GmbH &Co. KG, Germany) in the automated nucleic acid extractor
156 Maelstrom 4800 (TANBead Taiwan Advanced Nanotech Inc., Taiwan).

157

158 Identification of pathogen species was carried out by Polymerase Chain Reaction (PCR) of the genomic
159 DNA followed by amplicon sequencing of conserved nuclear locus, internal transcribed spacer (ITS)
160 rDNA. For ITS PCR, primer pair ITS1 (5'- TCCGTAGGTGAACCTGCGG-3') and ITS4 (5-
161 TCCTCCGCTTATTGATATGC-3') were used for genotyping (**White T.J., 1990**). PCR amplification
162 was followed by PCR clean-up using exonuclease kit (Thermo Fisher Scientific) according to the
163 manufacturer's instructions. Amplicons were subsequently sent for fragment sequencing at Macrogen
164 Europe (The Netherlands, https://www.macrogen-europe.com/). DNA sequences were manually
165 curated and analyzed for sequence homology to fungal sequences deposited at the National Center for
166 Biotechnology Information (NCBI) using the BLASTn search tool. Isolates used for leaf infection
167 assays were also tested with *F. graminearum* marker GOFW (5'-
168 ACCTCTGTTGTTCTTCCAGACGG-3') GORV (5'- CTGGTCAGTATTAACCGTGTGTG-3') (de
169 Biazio et al., 2008), and for *F. culmorum* with Fc03 (5'-TTCTTGCTAGGGTTGAGGATG-3') Fc02
170 (5'-GACCTTGACTTTGAGCTTCTTG-3') (**Astrid Bauer and Seigner, 2015**).

171

172 **Plant cultivation and infection assays**

173 Wheat plants were grown in the phytotron (controlled climate chambers) for three to four weeks at
174 20°C, 70% relative humidity and 300µMOL light intensity. The inoculum was composed of isolate
175 HK48 (*Fusarium graminearum*), HK50 (*Fusarium culmorum*). The isolates were incubated for two
176 weeks at 25°C and constant darkness on OMA. The conidia were scraped from the colony surface and
177 resuspended in sterile water. The inoculum cell density was adjusted to 250 spores per µl using water.
178 Leaf inoculation was based on a protocol originally developed at the Leibniz Institute of Plant Genetics
179 and Crop Plant Research and adapted to our conditions. Three- to four-weeks-old wheat leaves were
180 randomly selected and cut into 4 cm lengths. A hole was punctured in the middle of the leaf segment
181 and inoculated with a 30 µl spore suspension. Three biological replicates consisting of each of two
182 technical replicates were inoculated with either *F. graminearum* or *F. culmorum*. A total of 360 leaf
183 segments were placed in water agar and incubated in phytotron for four days. The necrosis was
184 observed in each of the 360 leaf segments and scored visually.

185

186 **Image analysis and morphotyping**

Isolate pictures were analyzed using the open-source Fiji from ImageJ (**Schindelin et al., 2012**). To minimize noise from the background, the region of interest (ROI) was defined manually with the circle tool and added to the ROI manager ("Analyze/Tools/ROI manager/Add" and "Edit/Clear outside"). Once the ROI was defined, general color data was extracted ("Analyzed/color histogram"). After this first step, the image was split into three different channels (blue, green, and red), and the different features of interest were extracted for each channel ("ROI manager/Measure"). To proceed with texture analysis of each channel image, we analyzed the image with the GLCM texture macro, defining the size of the step in pixels as 1 and the direction of the step as 0 degrees ("Plugins/GLCM texture"). Finally, the image type was changed to 32-bit ("Image/Type/32-bit") to perform the last step of the analysis. We selected *SurfCharJ1q* macro ("Plugins/ SurfCharJ1q") to analyze roughness features. At the end of the analysis, each sample had 90 different variables to be studied.

Statistical analysis

All statistical analyses were performed with R (version 4.2.2.) in Rstudio environment (**R Core Team, 2021**). The packages used for the analyses were: *caret, cluster, corrplot, datawizard, factoextra, faraway, readxl,* and *stats*. Data collected from ImageJ was normalized throughout the Z-scoring transformation. After data transformation, a linear model was adapted to analyze the putative correlation among the studied variables. Variables without changes among samples or with a correlation coefficient above 0.9 were removed. After this first filtering step, we performed a second selection, deleting variables with the highest correlation coefficients and variance inflation factors (VIF) values. Principal Component Analysis (PCA) was performed with the filtered and normalized data. To perform clustering analysis, agglomerative nesting (AGNES) and divisive analysis (DIANA) algorithms were applied for hierarchical clustering over our filtered data. Finally, *kmeans* and *medoids* analysis was performed with a predefined number of clusters of 2. *Kmeans* analysis was performed with *Hartigan* and *Wong* algorithm and Euclidean distance was selected for *medoids* analysis. The aggregation level of each cluster was measured throughout their silhouette value.

Results

Overall diversity of the wheat mycobiome library

In this study, hundreds of colonies were isolated from spikes and leaves collected over three field campaigns in eight counties across Sweden (Figure 1A). Of these, several isolates did not make it to the final set due to practical issues with growth, bacterial contaminations, failure of the genotyping at the PCR or the fragment-sequencing step. Still, we were able to recover a final set of 940 successfully genotyped samples which was the basis for the following analyzes. First, we concatenated all the genotypic data and evaluated the overall diversity of the resulting fungal collection in terms of genus diversity (Figure 1B). Here, it is important to read the following primarily in terms of qualitative diversity, considering the inherent bias due to the isolation method, and where abundance is primarily meant in terms of frequency of isolation. We were able to recover taxa from 14 different genera with a minimum of two representative (i.e. independently recovered isolates). Of these, the most abundant genera included *Fusarium* sp., the ubiquitous *Alternaria* sp., and to a lesser extent *Zymoseptoria* sp., *Pyrenophora* sp., *Microdochium* sp., and *Parastagonospora* sp., which is consistent with the fact that the sampling was mainly targeted to FHB, Leaf Blotch diseases of wheat. We therefore conclude that the resulting isolate library is relevant to the diseases covered by the survey.

We then assessed the species diversity of *Fusarium* sp. based on further analysis of ITS sequence specificity, markers, and colony morphology. Considering the limited species resolution we can obtain from ITS markers, even with all these approaches combined, frequencies must be here taken as an indication. We were able identify a several taxa typically associated with FHB in wheat, with the most common species including *F. culmorum*, *F. graminearum*, *F. poae*, and *F. avenaceum* (Figure 1C). We conclude that the collected data indicate a diversity of taxa typically implicated in head diseases of wheat present in Swedish wheat fields, representing a potential risk for disease outbreaks.

Finally, we assessed the overall diversity of the library in terms of the representation of disease-causing agents as well as potential antagonists potentially corresponding to candidate biological control agents. We reasoned that biological control agents often co-exist with their targets in the same ecological niches and may thus be co-isolated from the same tissues. To assign putative species name, we combined a series of classical pathological, symptom, and morphological criteria based on the observation of symptoms in the original material, and whenever possible, fruiting bodies, colony

246 morphology, and spore morphology. We were able to satisfactorily identify 16 different species. Of
247 these, 10 taxa correspond to pathogens commonly implicated in wheat diseases affecting the seeds, the
248 leaves, and the spikes, which is consistent with the wheat organs/tissues surveyed in this study (Table
249 1A, 1B). We also note that head blight and leaf blotch diseases are well represented in this list which
250 is again in line with the aim of this survey. Two putative species, *Nigrospora oryzae* and *Stemphylium*
251 *vesicarium*, have been described as potentially new wheat pathogens (**Liu et al., 2021, Mohamed et**
252 **al., 2022**), which we have classified as candidate emerging diseases for surveillance (Table 1B). We
253 also found four taxa that may represent potential biological control agents which were assigned based
254 on previous studies (Table 1C). We argue that such isolates represent an added value for the survey
255 aiding the identification of potentially beneficial microorganisms that could be evaluated for their
256 biological control properties.

257

258 **Inventory of pathogenic and endophytic isolates associated with Leaf Blotch in Sweden.**

259 For the leaf mycobiome associated with Leaf Blotch diseases, we recovered isolates from typical blotch
260 symptoms as well as from symptomless tissues. We deduced that symptomless tissues may be the
261 habitat for latent pathogens, endophytic fungi that could be antagonistic to the pathogenic, or harbor
262 pathogens surviving as silent endophytes.

263

264 Overall, *Alternaria* species dominated the infection, which is consistent with the fact that they are
265 known to be ubiquitously found as weak pathogens or saprophytes on different plant tissue (Figure
266 2A). *Alternaria* sp. apart, the most frequently isolated species were *Zymoseptoria* sp., *Pyrenophora*
267 sp., and *Parastagonospora* sp. Evidence from the symptoms where these taxa were isolated, combined
268 with colony morphology, and the observation of typical fruiting bodies indicated that the species are
269 *Zymoseptoria tritici*, *Pyrenophora tritici-repentis*, and *Parastagonospora nodorum*, respectively, all
270 of which being prominent causal agents of blotch diseases in wheat. We here conclude that the
271 collection isolated from leave does represent the diseases targeted by the survey. We then differentiated
272 the isolates recovered from typical blotch symptoms (Figure 2B), from those recovered from
273 symptomless tissues (Figure 2C). *Alternaria* sp. apart, *Zymoseptoria* sp., *Pyrenophora* sp., and
274 *Parastagonospora* sp were the most frequently isolated species from blotch symptoms, with further
275 symptomatic and morphological inspection indicated these isolates correspond to the species
276 *Zymoseptoria tritici*, *Pyrenophora tritici-repentis*, and *Parastagonospora nodorum*, respectively.

277

278 Interestingly, we have also isolated taxa typically implicated in FHB from the genera *Fusarium* sp. and
279 *Microdochium* sp.. Of these, several isolates had typical morphological attributes of *F. culmorum*, *F.*
280 *graminearum*, and *Microdochium nivale*. In comparison, the most frequently isolated taxa from
281 asymptomatic tissues apart from *Alternaria* sp. were *Pyrenophora* sp., and *Parastagonospora* sp., but
282 also *Zymoseptoria* sp. and *Microdochium* sp. This data suggest that members of the FHB complex can
283 possibly survive as latent pathogens or silent endophytes in the leaves and potentially cause blotch-like
284 symptoms that can be confound with the typical blotch pathogens *Z. tritici*, *P. tritici-repentis*, and *P.*
285 *nodorum*.

286

287 We then tested the capacity of *F. culmorum*, *F. graminearum* to cause blotch-like symptoms on wheat
288 leaves. To do so, we performed point inoculation of leaf segments harvested at the seedling stage and
289 visually assessed the development of necrotic lesions (see Methods). We inoculated 30 commercial
290 spring wheat cultivars commonly grown in Sweden (Figure 2D, 2E). We found that *F. culmorum*
291 caused necrotic lesions on at least 5 out of the 30 commercial cultivars tested (Figure 2D), while *F.*
292 *graminearum* caused necrotic lesions on 15 commercial cultivars (Figure 2E). These results
293 substantiate the hypothesis that *F. graminearum* and *F. culmorum* can potentially cause leaf blotch-
294 like symptoms in Swedish fields on several of the commonly grown spring wheat varieties.

295

296 **Inventory of pathogenic and endophytic isolates associated with FHB in Sweden**

297 For the spike mycobiome, we recovered isolates from seeds as well as from glumes and searched for
298 both pathogenic and non-pathogenic taxa. Our reasoning was that glumes may offer a secondary habitat
299 for wheat ear pathogens or potential antagonists competing for the same ecological niche in the seed
300 vicinity. In contrast to the leaf mycobiome, *Fusarium* species dominated over *Alternaria* sp. (Figure
301 3A). We then investigated the differences in the qualitative diversity between the taxa recovered from
302 seeds vs. glumes (Figure 3B, 3C). Interestingly, a much larger diversity of taxa was isolated from seeds,
303 while Fusarium sp. dominated in glumes as compared where a limited diversity of taxa was isolated
304 (Figure 3B, 3C). We also observed that *Fusarium* species fully occupy the seed habitat, with the glumes
305 possibly acting as a secondary niche where *Fusarium* sp. specifically seem to outcompete other fungal
306 taxa, such as *Alternaria* sp which has been isolated ubiquitously from all tissues analyzed in this study
307 except glumes.

We then expanded this analysis to possible differences between cultivars. We used a subset of samples recovered from a small propagation plot, where isolations were exclusively carried out with seeds. First, we concatenated the data by cultivar and genus with at least two representatives (Figure 3D), Additionally, we also included isolates from *Epicoccum* sp. which we could isolate from leaves, but also and mostly from seeds. Our reasoning was that *Epicoccum* sp. had been previously described as being associated with FHB, however, while a role as a possible antagonist/biocontrol agent has been suggested (**Karlsson et al., 2021**), its contribution to the FHB complex is still poorly understood. We found that *Alternaria* sp. could be isolated from most, if not all, cultivars, which is consistent with their characteristic as ubiquitous plant-associated fungi, sometimes acting as weak pathogens. However, the distribution of *Fusarium* sp. and *Epicoccum* sp. was more scattered across cultivars (Figure 3D).

We finally investigated the specific case of FHB-infected ears (Figure 3E) and leaves with typical blotch symptoms that were collected from the most northern location in our study: Piteå (Norrbotten county, Figure 1A). Interestingly, we mostly recovered *Michrodochium* sp. colonies (with typical features of *M. nivale*) from the leaf blotch symptoms and *F. avenaceum* and *Michrodochium* sp. from the FHB-infected ears (Figure 3G). These results suggest that in these northern latitudes, blotch symptoms can be probably caused by *Michrodochium* sp., which is the common agent of the Snow Mold disease of wheat, while FHB is possibly caused by the weaker pathogens *F. avenaceum* and *M. nivale*. We conclude that such observations demonstrate the usefulness of such surveys to shed light on possible changes in the disease landscape and alert on the possible re-emergence of diseases.

Morphotyping of *Fusarium* sp. and *Epicoccum* sp. isolates

In a last series of analyses, we took advantage of the library to explore the possibilities of morphotyping to rapidly sort and identify fungal species, with the prominent addition of modern image analysis technologies. We inferred that the capacity to rapidly sort and classify fungal taxa as soon as they are available as colonies growing on a plate will be a handy tool to accelerate and scale up the diagnostics, which would also allow us to target specific taxa or specific morphotypes. To do so, we aimed to provide a proof-of-concept using *Fusarium* sp. and *Epicoccum* sp. as targe taxa to differentiate solely using imaging.

339 A pipeline was designed to extract different image attributes from the isolate pictures using advanced
340 functions in the imageJ image analysis suite (see Methods). A Principal Component Analysis (PCA)
341 showed that although the subset of selected image variables still shows some level of correlation
342 (Figure 4A), they can still explain 56.7 % of the observed variability (Figure 4B). The image features
343 with the highest contribution to the '*Dimension 1*' is the mean blue channel, and the blue and green
344 intensity density (Figure 4C), meanwhile the highest contributors to 'Dimension 2' are the minimum
345 green intensity and the FAD values for red, blue, and green (Figure 4D). These results suggest that the
346 selected characteristics could represent a balanced mathematical description of the distribution of our
347 samples. However, we cannot exclude further optimization considering the inherent correlation
348 between some visual features (such as color) and the fact that some image features contribute more to
349 the total variability. Finally, with this still basic analysis, we could delineate two clear but slightly
350 overlapped clusters (Figure 4B) differentiating *Fusarium* sp. from *Epiccocum* sp. isolates. In order to
351 improve the clustering of our data, we applied Agglomerative Nesting (AGNES) (Figure 4E) and
352 Divisive Analysis Clustering (DIANA) (Figure 4F) algorithms (see Methods). The AGNES algorithm
353 resulted in a dendrogram with an agglomerative coefficient of 0.78; meanwhile, the DIANA algorithm
354 gave a higher value of 0.82, suggesting a solid clustering structure in our sample distribution. Although
355 the clustering does not differentiate between different *Fusarium* sp. species, the distribution shows that
356 we can reasonably differentiate between the genus *Epicoccum* sp. and *Fusarium* sp. with only six
357 miscalls.

358

359 Considering the quality of the data, we aimed at further clustering using *K-means* (Figure 5A) and
360 *Partition Around Medoids* (*PAM*) algorithms (Figure 5B), and calculated the average silhouette value
361 for each cluster created (Figure 5C, 5D). Although the global accuracy increased was improved to
362 0.918 (*K-means*) and 0.904 (*PAM*), we still had 6 miscalls with the *K-means* and 7 with the *PAM*,
363 which is consistent with the average silhouette value of 0.32 for the *K-means* clusters (Figure 5C) and
364 0.3 for the *PAM* clusters (Figure 5D). Interestingly, it seems that algorithms find it harder to
365 differentiate some *Epicoccum* sp. isolates from *Fusarium* sp. (*K-means*: 0.739, PAM: 0.739) while the
366 sensitivity for *Fusarium* (i.e. the capacity to properly identify *Fusarium* sp.) is higher in comparison
367 to *Epiccocum* (*K-means*: 0.980, PAM: 0.961. Therefore, despite the small dataset used in this analysis,
368 we could still provide proof of principle that imaging is a promising tool for advanced morphotyping
369 and the identification of specific fungi relevant to wheat.
370

371 **Discussion**

372 ***Wheat pathogens occupy a variety of tissues and niches***

373 In this study, we recovered typical wheat pathogens implicated in head blight and leaf blotch diseases
374 from a variety of tissues, including seeds, glumes, symptomatic leaf tissues, and asymptomatic leaves.
375 We had cases where *Fusarium* taxa typically implicated in FHB were isolated from blotch symptoms
376 in the leaves and other cases where typical blotch pathogens such as *P. tritici-repentis*, and *P. nodorum*
377 were isolated from wheat ears. Furthermore, typical leaf pathogens were also isolated as latent
378 pathogens or silent endophytes from asymptomatic tissues. Fusarium species are well known as
379 ubiquitous plant colonizers that can survive in a variety of plant tissues, and also in the soil (**Karlsson**
380 **et al., 2021**). In disease complexes such as FHB, where 17 different *Fusarium* and non-*Fusarium* taxa
381 can be implicated, the role of such secondary niches is poorly understood (**Karlsson et al., 2021**). From
382 a population perspective, the capacity of pathogens to survive in tissues or organs that are not their
383 primary habitat may increase the fitness of the pathogen population in the field by maintaining living
384 inoculum, throughout the field seasons and particularly when conditions are unfavorable. This was, for
385 instance, observed in the case of *Z. tritici*, where it was shown that avirulent isolates can still survive
386 and mate on resistant wheat hosts as symptomless endophytes or epiphytes (**Fones et al., 2023**), thus
387 contributing to pathogen fitness and adaptation through the maintenance of genetic diversity in the
388 field population. It was also shown that *Z. tritici* can induce systemic responses leading to whole plant
389 metabolic changes leading to increased susceptibility to secondary infection with a non-adapted
390 pathogen (**Seybold et al., 2020**). This is major because such mechanisms could also occur among
391 different isolates of the same pathogen population or different species of a disease complex, thus
392 providing a possible explanation for the functional relevance of secondary niches and the ubiquitous
393 nature of the taxa implicated in FHB.

394

395 ***The wheat mycobiome as a source for candidate biological control agents***

396 Microbial biological control agents are considered an important tool to reduce chemical inputs in crop
397 disease management. A variety of microbial agents with antagonistic properties against plant pathogens
398 has been described, and variety of mode of action underlying such effect has been reported including
399 antibiosis, parasitism, niche competition, or resistance priming in the host (**Köhl et al., 2019**).
400 Microbial biological control agents that correspond to naturally occurring competitors are commonly
401 found in the same ecological niches as their target pests. In this study, a few candidate biological control

402 agents have been identified (Table 1C). Of these, *Epicoccum* sp. have been shown to be a promising
403 biological control agent against wheat stripe rust as well as *F. graminearum*, while *Aureobasidium*
404 *pullulans* and *Meyerozyma guilliermondii* have been described as biological control agents against
405 post-harvest Fusarium crown rot diseases, respectively (**El-Sharkawy et al, 2023; Wachowska et al.,**
406 **2016; Kthiri et al., 2021**). These results further demonstrate the usefulness of such surveys in the
407 broader context of IPM, by facilitating the identification of relevant candidate biological control agents
408 better adapted to the Swedish conditions.

409

410 ***Wheat disease diagnostics and its importance for management***

411 The beneficial vs. pathogenic lifestyle of a plant colonizing fungus can be determined mainly by the
412 host and the ecological niches it occupies. For instance, the biological control fungus *Clonostachys*
413 *rosea*, a naturally occurring root endophyte, has been shown to be effective against several foliar plant
414 pathogens. However, *C. rosea* has also been reported as the causal agent of root rot, crown rot, and
415 wilt-type diseases in garlic, faba bean, avocado, strawberry, sugar beet, and medicinal plants such as
416 *Angelica sinensis* and *Astragalus mongholicus* (**Ma et al., 2020; Qi et al., 2022; Diaz et al., 2022;**
417 **Afshari et al., 2017; Coyotl-Pérez et al., 2007; Zhang et al., 2022; Haque and Parvin, 2020,**
418 **Farhaoui et al., 2023**). Similarly, *Epicoccum* sp. have been described as a potent biological control
419 agent against wheat stripe rust. However, *E. nigrum* is also the causal agent of the brown spot disease
420 in *Solanaceae* (**Jin et al., 2023**). These reports highlight the importance of continuous monitoring of
421 field populations and careful, systematic identification of the causal agents for identifying potential
422 lifestyle shifts in microbial populations.

423

424 Shifts from a beneficial endophytic lifestyle to pathogenicity through host switch, niche displacement,
425 and changes in the microbiome have been well documented for several prominent diseases such as
426 *Diplodia sapinea,* the causal agent of diplodia tip blight in Scots pine, and *Sarocladium oryzae* the
427 causal agent of rice sheet rot (**Blumenstein et al., 2022; Peeters et al., 2021**). Therefore, the
428 designation of beneficial endophyte/candidate biological control agents must be taken within the
429 context of the actual contribution of the species to the wheat mycobiome, meaning that both disease-
430 suppressing antagonistic and disease-promoting synergistic properties must be tested. This is directly
431 relevant to taxa such as *Epicoccum* sp. and *Alternaria* sp., considering their frequent association with

432 FHB and our poor understanding of how such mycobiome is assembled (**Karlsson et al., 2021; Schiro**
433 **et al., 2018; Nazabanita et al., 2022; Rojas et al., 2020**).

434

435 In this context, changes in the composition of the disease complex are also relevant, with the example
436 of FHB from Piteå, which seems to be caused by *F. avenaceum* and *M. nivale* (Figure 3F, 3G) and not
437 by *F. graminearum* and *F. culorum* as in the majority of the FHB tested samples (Figure 3A, 3B, 3C).
438 In contrast, we also recovered those typical FHB causal agents, *F. graminearum* and *F. culorum*, from
439 typical necrotic and chlorotic symptoms reminiscent of septoria leaf blotch diseases. These results
440 highlight the complexity of the wheat mycobiome and the limits of visual scoring considering the
441 complexity and often the convergence of disease symptoms caused by yet phylogenetically distant
442 taxa. We argue that such observations further highlight the importance of field surveys as a tool for
443 continuous identification and re-identification of the actual disease-causing agents present in the field.

444

445 ***A basis for targeted monitoring of potentially emerging wheat diseases***

446 The emergence of new diseases leading to global epidemics is relatively common in wheat, with stem
447 rust and wheat blast being two prominent examples. Wheat has also been the host for the emergence
448 of two new pathogens that did not existence before namely triticale powdery mildew and wheat blast.
449 Arguably, the large reservoir of wheat pathogens present in the agro-ecosystem is a challenge requiring
450 continuous monitoring for early detection of potentially new, emerging diseases. In this context, two
451 taxa identified in our survey are of particular interest: *N. oryzae*, and *S. vesicarium* (Table 1B). *N.*
452 *oryzae* is an ascomycete fungal pathogen and the causal agent of panicle branch rot disease on rice
453 (*Oryza sativa*) (**Liu et al., 2021**) In 2016, *N. oryzae* was reported to cause black lesions on the
454 hypocotyls of wheat seedlings in Kazakhstan, suggesting that some isolates of *N. oryzae* (a rice
455 pathogen) may have adapted to be pathogens on wheat, which is reminiscent of the emergence of wheat
456 blast (**Eken et al., 2016**). Similarly, *S. vesicarium* has been reported to cause leaf spots on wheat in
457 Egypt (**Mohamed et al., 2022**), and to our knowledge, these pathogens have never been described in
458 Sweden before. We conclude that such results further highlight the relevance of this work since we can
459 now provide a rational basis for risk assessment and targeted disease monitoring of critical pathogens
460 in Swedish wheat fields.

461

462 **Author Contributions**

463 SB and HV led the research. SB, HZ, and JZ designed the research and developed the library. HK, EV,
464 MACG, HV, SB did laboratory experiments. HK, MACG, SB, DD, and FD developed infection assays.
465 MACG and SB developed the morphotyping. HK, EV, HV, and SB analyzed the genotyping data.
466 MACG performed statistical analyzes. MACG and SB edited the figures.

467

468 **Funding**

469 This was supported by funding from the Swedish Research Council for Sustainable Development
470 FORMAS (grant number 2020-01007) and the Carl Trygger Foundation (grant number 21:1171).

471 **Acknowledgments**

472 We would like to acknowledge the support of the Plant Protection Extensions 'Växtskyddscentralerna'
473 of the Swedish Board of Agriculture 'Jordbruksverket' (https://jordbruksverket.se/) with field sampling
474 across Sweden. We would like to thank Anders Lindgren, Lina Norrlund, and Elizabeth Lovetta for
475 supporting and coordinating sample collection and shipment. We thank Eula Gems Oreiro, Björn
476 Andersson from the Department of Forest Mycology and Plant Pathology (SLU) for their help handling
477 blotch infected samples and their contribution to maintaining the library. We also thank Fredric
478 Hedlund and Ayano Tanaka for their technical assistance with the growth facilities and the SLU
479 BioCentrum. We finally thank Katarina Ihrmark and Maria Jonsson for their technical assistance.

480

481

482 **Figures**

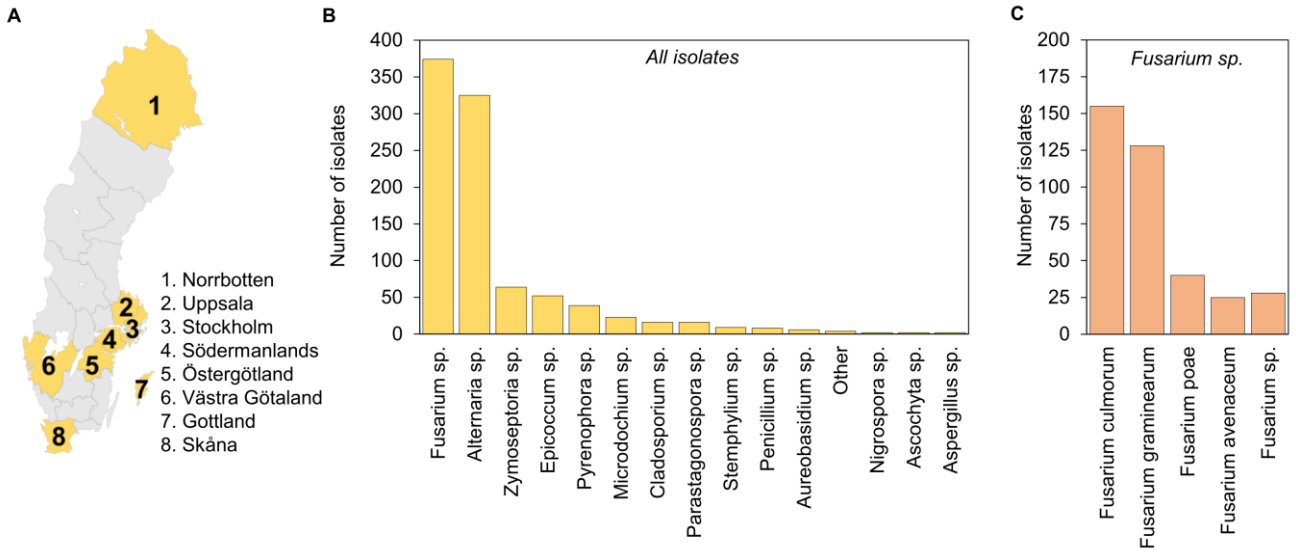

483

484 **Figure 1**. Summary and overall diversity of the wheat mycobiome library

485 (A) Geographical origin of the samples. (B) Overall diversity of the fungal genera represented in the library. (C)
486 Partial analysis of species diversity of *Fusarium* sp.

487

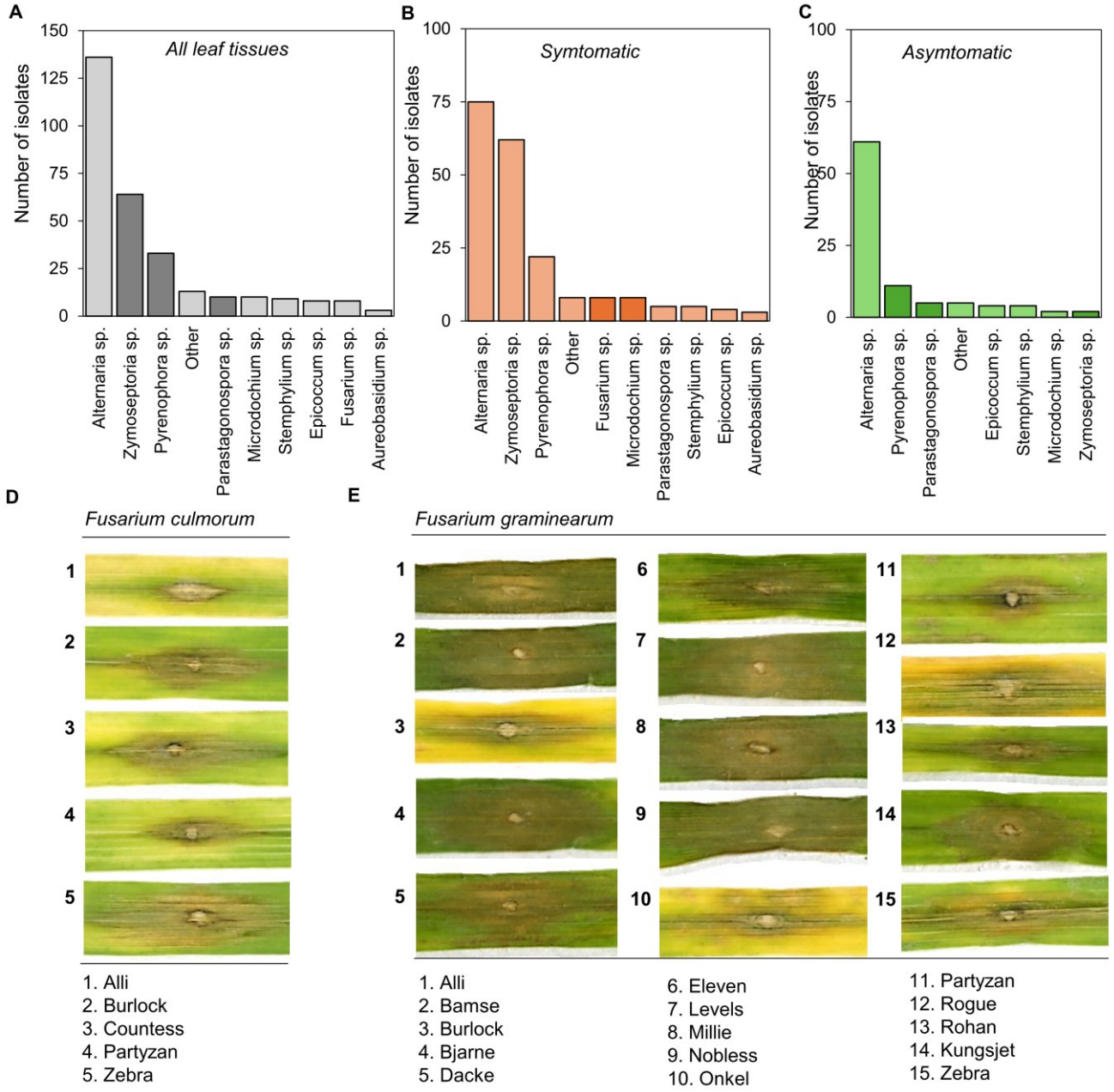

Figure 2. Summary of the wheat leaf mycobiome

(A) Overall diversity of the fungal taxa isolated from leaf tissues. (B) Summary of the fungal taxa recovered from tissues with typical leaf blotch symptoms. (C) Summary of the fungal taxa recovered from asymptomatic tissues from leaf blotch infected material. (D) Point leaf inoculations of different spring wheat commercial cultivars with *Fusarium culmorum* (see Methods). (E) Point leaf inoculations of different spring wheat commercial cultivars with *Fusarium graminearum* (see Methods).

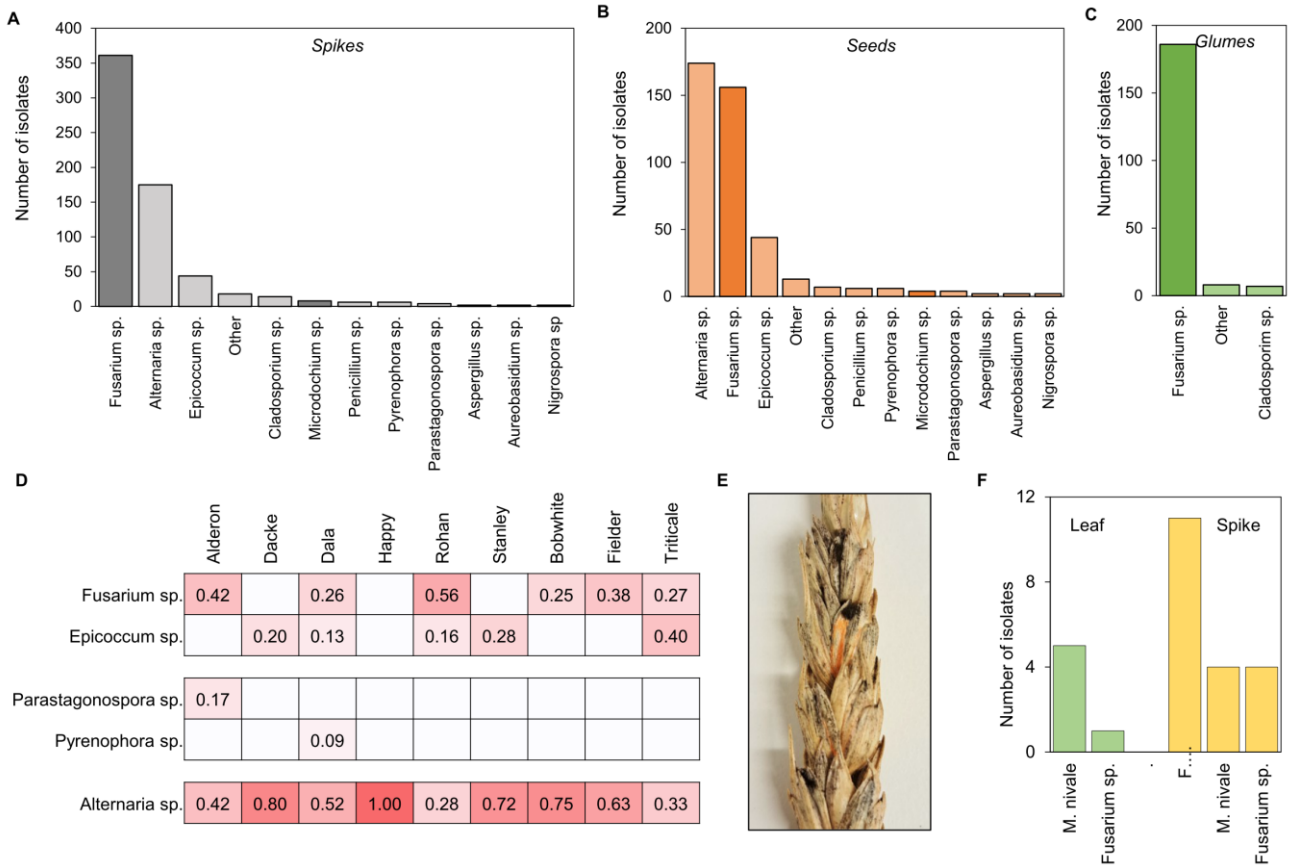

Figure 3. Summary of the wheat head mycobiome

(A) Overall diversity of the fungal taxa isolated from spikes. (B) Summary of the fungal taxa recovered from seeds. (C) Summary of the fungal taxa recovered from glume tissues. (D) Analysis of possible association between fungal taxa and wheat cultivars. (E) Photograph of typical Fusarium Head Blight symptoms on a wheat spike collected from the most northern location in our survey: Piteå. (F) Summary of the fungal taxa isolated from typical leaf blotch and head blight symptoms from samples collected in Piteå.

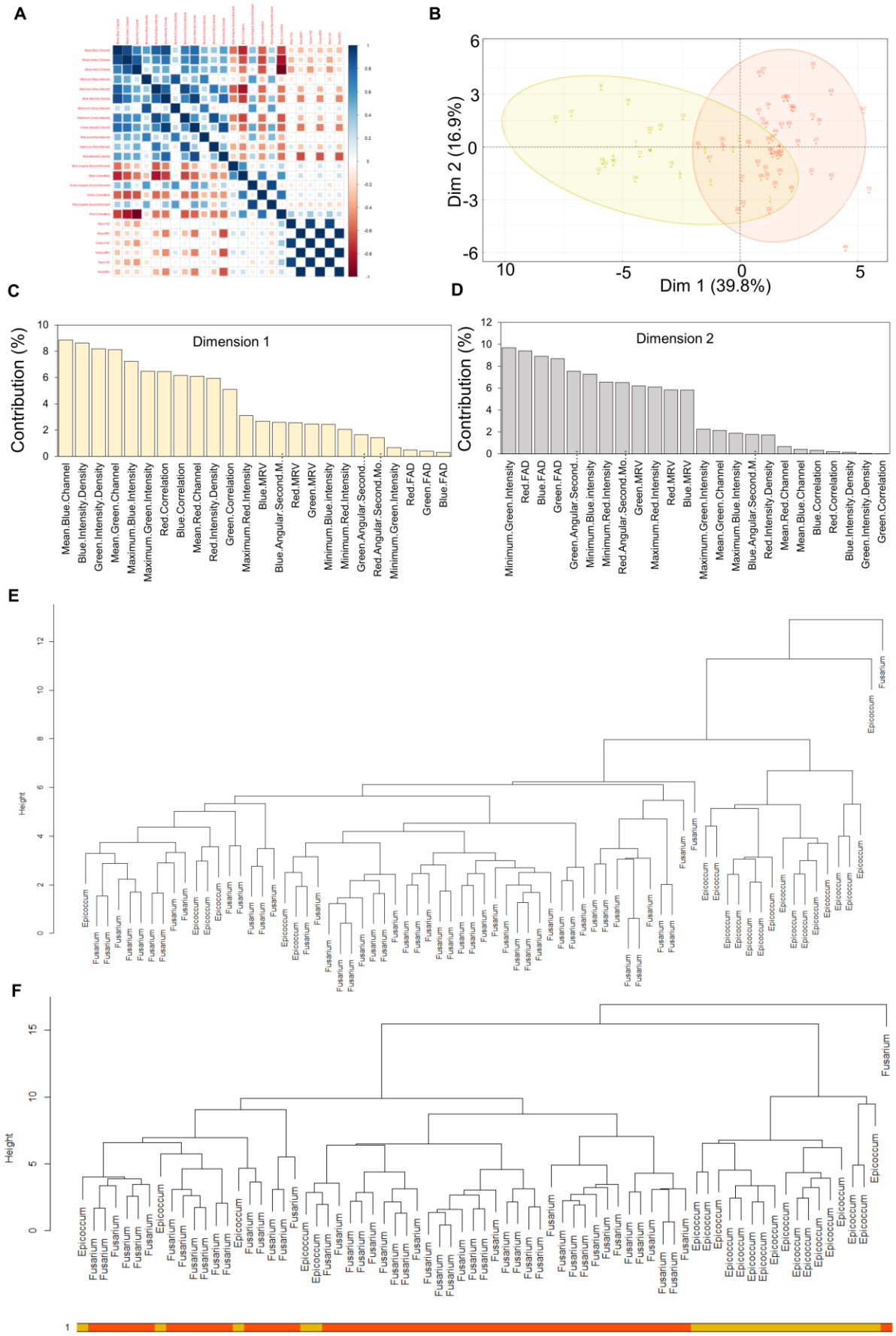
A
B
Dim 2 (16.9%)
Dim 1 (39.8%)
C
Dimension 1
Contribution (%)
Mean.Blue.Channel
Blue.Intensity.Density
Green.Intensity.Density
Mean.Green.Channel
Maximum.Blue.Intensity
Maximum.Green.Intensity
Red.Correlation
Blue.Correlation
Mean.Red.Channel
Red.Intensity.Density
Green.Correlation
Maximum.Red.Intensity
Blue.MRV
Blue.Angular.Second.M...
Red.MRV
Green.MRV
Minimum.Blue.intensity
Minimum.Red.Intensity
Green.Angular.Second...
Red.Angular.Second.Mo...
Minimum.Green.Intensity
Red.FAD
Green.FAD
Blue.FAD
D
Dimension 2
Contribution (%)
Minimum.Green.Intensity
Red.FAD
Blue.FAD
Green.FAD
Green.Angular.Second...
Minimum.Blue.intensity
Minimum.Red.Intensity
Red.Angular.Second.Mo...
Green.MRV
Maximum.Red.Intensity
Red.MRV
Blue.MRV
Maximum.Green.Intensity
Mean.Green.Channel
Maximum.Blue.Intensity
Blue.Angular.Second.M...
Red.Intensity.Density
Mean.Red.Channel
Mean.Blue.Channel
Blue.Correlation
Red.Correlation
Blue.Intensity.Density
Green.Intensity.Density
Green.Correlation
E
Height
Epicoccum
Fusarium
F
Height
Epicoccum
Fusarium

504

505 **Figure 4.** Feature extraction for morphotyping and dendrogram classification

506 (A) Correlation matrix of selected variables for image analysis of *Epicoccum* sp. and *Fusarium* sp. blue color
507 (values close to 1) indicates positive correlation meanwhile red color indicates negative correlation. (B) Principal
508 component analysis plot of visual data extracted from *Epicoccum* sp. and *Fusarium* sp. Isolate images. The
509 color yellow represents *Epicoccum* sp. isolates, and the red color represents *Fusarium* sp. isolates. Circles
510 represent putative clusters. Dimension 1 and dimension 2 separate isolates based in the values of 24 different
511 visual characteristics. (C) Weights of the main explanatory variables for the first PCA dimension. (D) Weights of
512 the main explanatory variables for the second PCA dimension. (E) Dendrogram clustered by AGNES algorithm
513 built with Unweighted Pair Group Method with Arithmetic Mean (UPGMA). (F) Dendrogram clustered by the
514 DIANA algorithm. The yellow color represents *Epicoccum* sp. isolates, and the red color indicates *Fusarium* sp.
515 isolates.
516

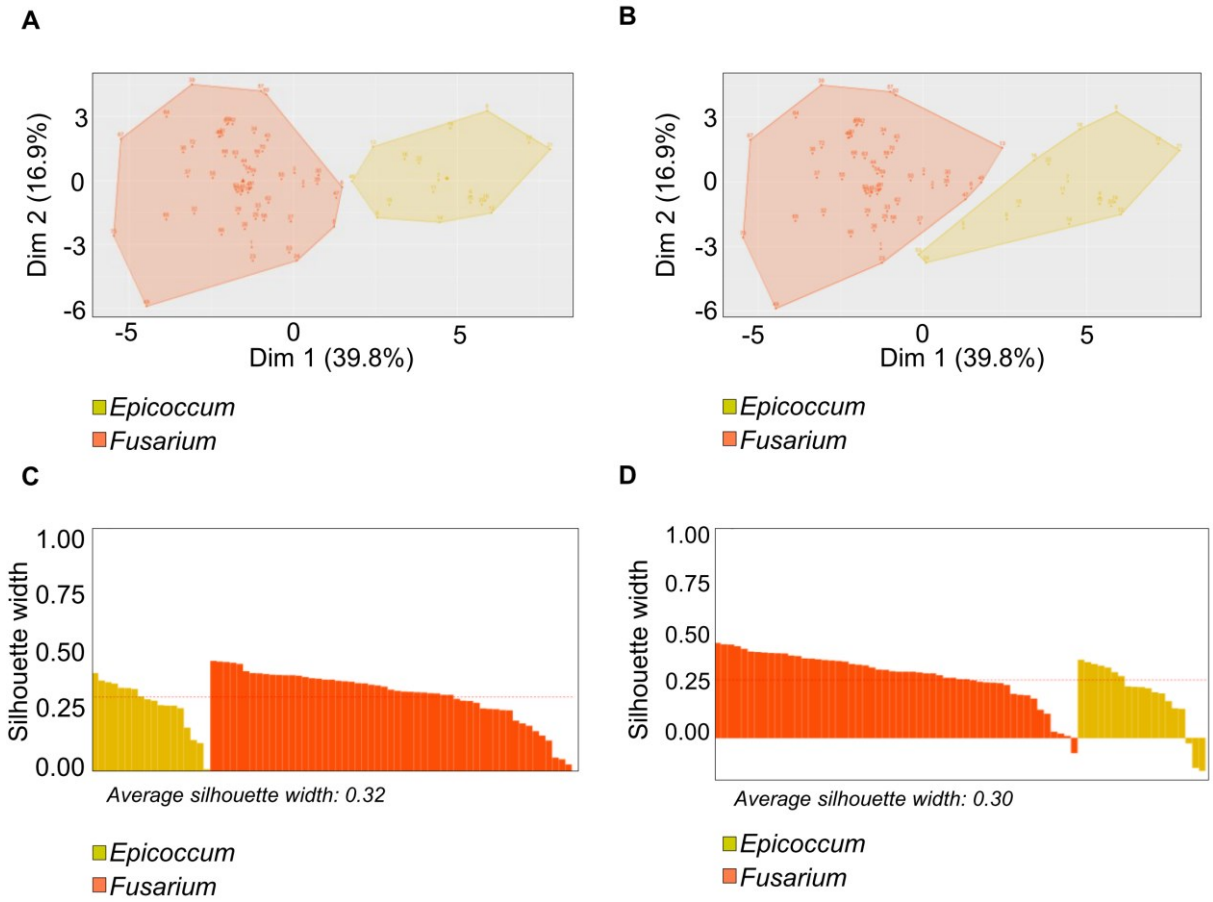

Figure 5. K-mean and PAM clustering of *Epicoccum* sp. and *Fusarium* sp. isolates

(A) Cluster analysis performed by K-means algorithm. The pre-selected number of clusters was defined as 2. Yellow represents the putative cluster for *Epicoccum* sp. isolates and red color represents the putative cluster for *Fusarium* sp. (B) Cluster analysis performed by PAM algorithm. The number of clusters was predefined as 2. Yellow area represents *Epicoccum* sp. isolates and the red area shows *Fusarium* sp. (C) Silhouette values for each isolate and average silhouette from cluster analysis with the K-means algorithm. (D) Silhouette values for each isolate and average silhouette from cluster analysis with the PAM algorithm. In (C) and (D) samples aggregated as *Epicoccum* sp. are represented with yellow bars meanwhile samples aggregated as *Fusarium* sp. are represented as red bars.

528 **Tables**

529 **Table 1.** Summary of possible contributions of different taxa to the wheat mycobiome.

Species	Predicted contribution	Reference
A. *Common wheat pathogens*		
Alternaria alternata	Black point	Somma et al. (2019)
Alternaria infectoria	Black point	Somma et al. (2019)
Fusarium avenaceum	Head blight	Karlsson et al. (2021)
Fusarium culmorum	Head blight	Karlsson et al. (2021)
Fusarium graminearum	Head blight	Karlsson et al. (2021)
Fusarium poae	Head blight	Karlsson et al. (2021)
Microdochium nivale	Fusarium Head Blight	Karlsson et al. (2021)
Parastagonospora nodorum	Septoria nodorum blotch	Bertazzoni et al. (2021)
Pyrenophora tritici-repentis	Tan spot	Moolhuijzen et al. (2022)
Zymoseptoria tritici	Septoria tritici blotch	Goodwin et al. (2011)
B. *Potentially emerging diseases*		
Nigrospora oryzae	Seed pathogen	Eken et al. (2016)
Stemphylium vesicarium	Leaf spot	Farag et al. (2022)
C. *Candidate biological control agents*		
Aureobasidium pullulans	Beneficial | Antagonist	Wachowska et al. (2014)
Epicoccum nigrum	Beneficial | Antagonist	Ogorek et al. (2011)
Meyerozyma guilliermondii	Beneficial | Antagonist	Kthiri et al. (2021)
Penicillium chrysogenum	Beneficial | Antagonist	Barna et al. (2008)

530

531

532 **References**

533 Karlsson, I., Persson, P., Friberg, H. (2021). Fusarium head blight from a microbiome perspective.
534 *Front. Microbiol*. 12, 628373. doi: 10.3389/fmicb.2021.628373.

535 Xu, X.M., Parry, D.W., Nicholson, P. *et al.* (2005). Predominance and association of pathogenic
536 fungi causing Fusarium ear blightin wheat in four European countries. *Eur. J. Plant Pathol* 112,
537 143–154. doi: 10.1007/s10658-005-2446-7

538 Brown, J. K., Chartrain, L., Lasserre-Zuber, P., Saintenac, C. (2015) Genetics of resistance to
539 *Zymoseptoria tritici* and applications to wheat breeding. *Fungal Genet. Biol*. 79, 33-41. doi:
540 10.1016/j.fgb.2015.04.017.

541 Pereira, D., McDonald, B. A., Croll, D. (2020) The genetic architecture of emerging fungicide
542 resistance in populations of a global wheat pathogen. *Genome Biology and Evolution*, 12, 2231-
543 2244, doi: 10.1093/gbe/evaa203

544 Justesen, A.F., Corsi, B., Ficke, A. *et al.* (2021) Hidden in plain sight: a molecular field survey of
545 three wheat leaf blotch fungal diseases in North-Western Europe shows co-infection is
546 widespread. *Eur. J. Plant Pathol.* 160, 949–962. doi: 10.1007/s10658-021-02298-5

547 Jørgensen, L.N., Matzen, N., Heick, T.M. *et al.* (2018). Decreasing azole sensitivity of *Z. tritici* in
548 Europe contributes to reduced and varying field efficacy. *J. Plant Dis. Prot.* 128, 287-301. doi:
549 10.1007/s41348-020-00372-4

550 Jørgensen, L.N., Matzen, N., Heick, T.M., O'Driscoll, A., Clark, B., Waite, K., Blake, J., Glazek, M.,
551 Maumene, C., Couleaud, G., Rodemann, B., Weigand, S., Bataille, C. R. B., Hellin, P., Kildea, S.
552 and Stammler, G. (2022) Shifting sensitivity of septoria tritici blotch compromises field
553 performance and yield of main fungicides in Europe. *Front. Plant Sci*. 13:1060428. doi:
554 10.3389/fpls.2022.1060428.

555 Singh, r. V., Hodson, D. P., Huerta-Espino, J., Jin, Y., Bhavani, S., Njau, P., Herrera-Foessel, S.,
556 Singh, P. K., Singh, S., Govindan, V. (2011). *Annu. Rev. of Phytopathol*. 49, 465-481. doi:
557 10.1146/annurev-phyto-072910-095423

558 Patpour, M., Hovmøller, M.S., Rodriguez-Algaba, J., Randazzo, B., Villegas, D., Shamanin, V.P.,
559 Berlin, A., Flath, K., Czembor, P., Hanzalova, A., Sliková, S., Skolotneva, E.S., Jin, Y., Szabo, L.,
560 Meyer, K.J.G., Valade, R., Thach, T., Hansen, J.G. and Justesen, A.F. (2022) Wheat stem rust

561 back in europe: diversity, prevalence and impact on host resistance. *Front. Plant Sci*. 13:882440.
562 doi: 10.3389/fpls.2022.882440

563 Menardo, F., Praz, C., Wyder, S. *et al.* (2016) Hybridization of powdery mildew strains gives rise to
564 pathogens on novel agricultural crop species. *Nat. Genet.* **48**, 201-205. doi: 10.1038/ng.3485.

565 Huang, S., Pang, F. (2017). Biocontrol agents for controlling wheat rust. In: Periyannan, S. (eds)
566 Wheat rust diseases. *Methods Mol. Biol*. 1659. Humana Press, New York, NY. doi: 10.1007/978-
567 1-4939-7249-4-24

568 Yue, H.M., Wang, M., Gong, W-F., Zhang, L-Q. (2018) The screening and identification of the
569 biological control fungi *Chaetomium* spp. against wheat common root rot, *FEMS Microbiol.*
570 *Letters.* 365, fny242. doi: 10.1093/femsle/fny242

571 Rojas, E.C:, Jensen, B:, Jørgensen, H.J.L. Latz, M.A.C., Esteban, P., Ding, Y., Collinge, D.B. (2020).
572 Selection of fungal endophytes with biocontrol potential against Fusarium head blight in wheat.
573 *Biological Control*, 144, 104222. doi: 10.1016/j.biocontrol.2020.104222.

574 Fagundes, W. C.; Haueisen, J., Stukenbrock, E.H. (2020). Dissecting the biology of the fungal wheat
575 pathogen *Zymoseptoria tritici*: a laboratory workflow. *Curr. Protocols in Microbiol*. 59, e128. doi:
576 10.1002/cpmc.128

577 White, T.J. (1990) Amplification and direct sequencing of fungal ribosomal RNA genes for
578 phylogenetics. In: PCR Protocols, a Guide to Methods and Applications, 315-322.
579 doi:10.1016/B978-0-12-372180-8.50042-1

580 de Biazio, G.R., Leite, G.G., Tessmann, D.J., Barbosa-Tessmann, I.P. (2008) A new PCR approach
581 for the identification of *Fusarium graminearum*. *Braz. J. Microbiol*. 39, 554-60. doi:
582 10.1590/S1517-838220080003000028.

583 Astrid Bauer, R.S., Seigner, L. (2015). Detection, identification and quantification of *Fusarium*
584 *graminearum* and *Fusarium culmorum* in wheat kernels by PCR techniques. *Jour. Plant Pathol.*
585 *Microbiol*. 6, 7. doi: 10.4172/2157-7471.1000287

586 Schindelin, J., Arganda-Carreras, I., Frise, E. et al. (2012) Fiji: an open-source platform for
587 biological-image analysis. *Nat Methods* 9, 676–682. doi: 10.1038/nmeth.2019

588 R Core Team (2021). R: A language and environment for statistical computing. R Foundation for
589 Statistical Computing, Vienna, Austria. URL https://www.R-project.org/

590 Liu, L., Zhao, K., Zhao, Y., Zhang, Y., Fu, Q., Shiwen, H. (2021) *Nigrospora oryzae* causing panicle
591 branch rot disease on *Oryza sativa* (rice). *Plant Dis.* 105, doi: 10.1094/PDIS-11-20-2423-PDN.

592 Mohamed, M.E. (2022) Detection and molecular diagnosis of Stemphylium vesicarium isolated from
593 wheat spikes. *Egypt. Jour. Phytopath*. 50, 63-68. doi: 10.21608/ejp.2022.166572.1072.

594 Fones, H.N., Soanes, D., Gurr, S.J. (2023) Epiphytic proliferation of *Zymoseptoria tritici* isolates on
595 resistant wheat leaves. Fung. Genet. Biol. 168, 103822. doi: 10.1016/j.fgb.2023.103822.

596 Seybold, H., Demetrowitsch, T.J., Hassani, M.A. *et al.* (2020) A fungal pathogen induces systemic
597 susceptibility and systemic shifts in wheat metabolome and microbiome composition. *Nat.*
598 *Commun.* 11, 1910. doi: 10.1038/s41467-020-15633-x

599 Köhl, J., Kolnaar, R. and Ravensberg, W.J. (2019) Mode of action of microbial biological control
600 agents against plant diseases: relevance beyond efficacy. *Front. Plant Sci.* 10:845. doi:
601 10.3389/fpls.2019.00845

602 El-Sharkawy, H.H.A., Rashad, Y.M., Elazab, N.T. (2023) Biocontrol potential of the endophytic
603 *Epicoccum nigrum* HE20 against stripe rust of wheat. *Pestic. Biochem. Physiol*. 194, 05517. doi:
604 10.1016/j.pestbp.2023.105517

605 Wachowska, U., Głowacka, K., Mikołajczyk, W. et al. (2016) Biofilm of *Aureobasidium pullulans*
606 var. *pullulans* on winter wheat kernels and its effect on other microorganisms. *Microbiol.* 85, 523–
607 530. doi: 10.1134/S0026261716050192

608 Kthiri, Z., Jabeur, M. B., Chairi, F., López-Cristoffanini, C., López-Carbonell, M., Serret, M. D.,
609 Araus, J. L., Karmous, C., Hamada, W. (2021) Exploring the potential of *Meyerozyma*
610 *guilliermondii* on physiological performances and defense response against Fusarium crown rot on
611 durum wheat. *Pathogens* 10, 52. doi: 10.3390/pathogens10010052

612 Ma, H., Duan, X., Xu, W., Ma, G., Ma, W., Qi, H. (2022) Root rot of *Angelica sinensis* caused by
613 *Clonostachys rosea* and *Fusarium acuminatum* in China. *Plant Dis.* 106:8, 2264. doi:
614 10.1094/PDIS-12-21-2665-PDN

615 Hexing Qi, Xiaoming Duan, Wenhua Xu, Yuantao Zhou, Haixia Ma, Weili Ma, and Guihua Ma
616 (2022) First report disease of *Clonostachys rosea* causing root rot on *Astragalus membranaceus* in
617 China. *Plant Dis.* 106, 6. doi: 10.1094/PDIS-07-21-1511-PDN

618 Diaz, R., Chavez, E.C., Delgado Ortiz, J.C., Velazquez, J.J., Roque, A., Ochoa, Y.M. (2022) First
619 report of *Clonostachys rosea* causing root rot on garlic in Mexico. *Plant Dis*. 106:11 doi:
620 10.1094/PDIS-12-21-2658-PDN.

621 Afshari, N., Hemmati, R. (2017) First report of the occurrence and pathogenicity of *Clonostachys*
622 *rosea* on faba bean. *Australasian Plant Pathol*. 46, 231-234 doi:10.1007/s13313-017-0482-3

623 Coyotl-Pérez, W.A., Romero-Arenas, O., Mosso-González, C., Pacheco-Hernández, Y., Rivera-Tapia
624 J.A., Villa-Ruano, N. (2022) First report of *Clonostachys rosea* associated with avocado fruit rot
625 in Puebla, Mexico. *Rev. Mex. Phytopathol* 40, 298-307. doi: 10.18781/r.mex.fit.2203-5

626 Zhang, Y., Yu, H., Hu, M., Wu, J., Zhang, C. (2022) Fungal pathogens associated with strawberry
627 crown rot disease in china. *J. Fungi* 8, 1161. doi:10.3390/jof8111161

628 Haque, M.E. and Parvin, M.S. (2020) First report of *Clonostachys rosea* causing root rot of *Beta*
629 *vulgaris* in North Dakota, USA. *New Disease Reports*, 42, 21-21. doi: 10.5197/j.2044-
630 0588.2020.042.021.

631 Farhaoui, A., Tahiri, A., Radouane, N., Khadiri, M., Amiri, S., El Alami, N. et al. (2023) First report
632 of *Clonostachys rosea* causing sugar beet root rot in Morocco. *New Disease Reports*, 48, e12235.
633 doi: 10.1002/ndr2.12235

634 Jin, M., Yang, C., Wang, Y., Wei, L. & Osei, R. (2023) Isolation and identification of *Epicoccum*
635 *nigrum* as the causal agent of brown spot disease in *Solanum tuberosum* in China. *Plant Pathol*.
636 72, 829-838. doi: 10.1111/ppa.13696.

637 Blumenstein, K., Bußkamp, J., Langer, G.J., Terhonen, E. (2022) Diplodia tip blight pathogen's
638 virulence empowered through host switch. *Front. Fungal Biol*. 3: 939007. doi:
639 10.3389/ffunb.2022.939007

640 Peeters, K.J., Audenaert, K., Höfte, M. (2021) Survival of the fittest: how the rice microbial
641 community forces *Sarocladium oryzae* into pathogenicity. *FEMS Microbiol. Ecol*. 97:fiaa253. doi:
642 10.1093/femsec/fiaa253

643 Schiro, G., Verch, G., Grimm, V., Müller, M.E.H. (2018) Alternaria and Fusarium fungi: differences
644 in distribution and spore deposition in a topographically heterogeneous wheat field. J. Fungi 4:63.
645 doi: 10.3390/jof4020063.

646 Nzabanita, C., Zhang, L., Zhao, H., Wang, Y., Wang, Y., Sun, M., Wang, S., Guo, L. (2022) Fungal
647 endophyte *Epicoccum nigrum* 38L1 inhibits in vitro and in vivo the pathogenic fungus *Fusarium*
648 graminearum. *Biological Control* 174: 397-408. doi: 10.1016/j.biocontrol.2022.105010.

649 Rojas, E.C., Sapkota, R., Jensen, B., Jørgensen, H.J.L., Henriksson, T., Jørgensen, L.N., Nicolaisen,
650 M., Collinge, D.B. (2020) Fusarium head blight modifies fungal endophytic communities during
651 infection of wheat spikes. *Microb. Ecol.* 79:397-408. doi: 10.1007/s00248-019-01426-3

652 Eken, C., Spanbayev, A., Tulegenova Z., Yechshzhanov, T. (2016) First report of *Nigrospora oryzae*
653 on wheat in Kazakhstan. *Plant Dis*. 4:861-861. doi: 10.1094/PDIS-08-15-0915-PDN.

654

655